Journal of Solid Mechanics Vol. 6, No. 1 (2014) pp. 70-81

Free Vibration Analysis of Orthotropic FGM Cylinders by a Mesh-Free Method

R. Moradi-Dastjerdi[1], M. Foroutan[2,*]

[1]*Young Researchers and Elite Club, Khomeinishahr Branch, Islamic Azad University, Khomeinishahr, Iran*
[2]*Department of Mechanical Engineering, Razi University, Kermanshah, Iran*

Received 28 September 2013; accepted 14 December 2013

ABSTRACT

In this paper, free vibration analysis of orthotropic functionally graded material (FGM) cylinders was carried out by a Mesh-Free method. In this analysis, moving least squares shape functions are used for approximation of displacement field in the weak form of equilibrium equation. Essential boundary conditions are imposed by transformation method. In this simulation, an axisymmetric model is used. The orthotropic FGM cylinders are assumed to be a mixture of two isotropic materials as fiber and matrix. The volume fraction of the fiber is changed in the radial direction. Consequently, mechanical properties of these cylinders are changed in the radial direction. Free vibration analysis of orthotropic FGM cylinders with any arbitrary combination of boundary conditions is possible by the proposed model. Natural frequencies obtained from the presented model are in good agreement with results of finite element simulation and other results from literature. Effects of various types of boundary conditions, geometrical parameters, and mechanical properties on the natural frequencies are studied.

Keywords: FGM; Orthotropic; Mesh-free, Axisymmetric; Free vibration

1 INTRODUCTION

FUNCTIONALLY graded materials were introduced for the first time by the material scientists as heat resistant materials for using in space planes and nuclear reactors [1]. Recently, large amount of researches about application of these materials in wide range of industries such as dental and orthopedic implants, energy conversion, heat generators and sensors have been carried out. Additional potential applications of FGMs include their using as interfacial zones to improve the bonding strength and to reduce residual stresses in bonded dissimilar materials and as wearing resistant layers such as gears, cams ball and roller bearings and machine tools [2]. FGMs are inhomogeneous composite materials with gradient compositional variation of the constituents (e.g., metal and ceramic) from one surface of the material to the other, which results in continuously varying material properties. Therefore FGMs have a non uniform microstructure and a continuously variable macrostructure.

Recently, several researches have been carried out on free vibration analysis of FGM cylinders. Loy et al. [3] analyzed free vibration of FGM cylinders by using Love's first-approximation theory and Ritz method. They studied the effects of volume fraction exponent and boundary conditions on the natural frequencies of these cylinders. In a similar work Pradhan et al. [4] the effect of material properties on the natural frequencies of FGM cylindrical shells. Kadoli and Ganesan [5] simulated thermal buckling and free vibration of FGM cylinders using first-order shear deformation theory and Fourier series expansion of displacement field in circumferential direction. Haddadpour et

* Corresponding author. Tel.: +98 831 4274536; Fax: +98 831 427 4542.
E-mail address: Foroutan@razi.ac.ir (M. Foroutan).

al. [6] analyzed free vibrations of simply supported FGM cylinders with thermal dependent material properties by the Galerkin method. Ansari and Darvizeh [7] presented an analytical solution for free vibrations of FGM cylinders using first-order shear deformation theory. They studied effects of boundary conditions and volume fraction exponent on natural frequencies. Mollarazi et al. [8] analyzed free vibration of FGM cylinders by the Mesh-Free method that is used in this paper, but they considered isotropic FGM cylinders while in this paper, orthotropic property of FGM cylinders are considered. Also several analyses have been carried out concerning free vibrations of isotropic homogeneous cylinders. Among these analyses Leissa and So [9,10] and Hutchinson [11,12] used the Rayleigh-Ritz method and Zhou et al. [13] used the Chebyshev-Ritz method in their analyses.

Also several researches have been carried out about dynamic analysis and stress wave propagation in the FGM cylinders. Han et al. [14] analyzed transient waves in FGM cylinders using a hybrid numerical method (HNM). Shakeri et al. [15] analyzed radial wave propagation in FGM cylinders with infinite length by FEM and Newmark method. They considered the FGM cylinder as a multilayer cylinder with constant material property for each layer. Hosseini et al. [16] analyzed the same problem considering variable material property in the layers. Asgari et al. [17] carried out analysis of cylinders with variable material property in radial and axial directions (2D FGM) by FEM and Newmark method. Hosseini and Abolbashiri [18] presented an analytical solution for FGM cylinders with infinite length subjected to an impact load. Shahabian and Hosseini [19] carried out stochastic dynamic analysis under the impact load by FEM. Among the few works, about the wave propagation in FGMs by mesh-free methods, Zhang and Batra's work [20] can be mentioned. They analyzed wave propagation in a FGM plate by modified smoothed particle hydrodynamics (MSPH) method. Static and dynamic analysis and stress wave propagation of FGM cylinders under an impact load and also, dynamic analysis of nanocomposite cylinders was carried out by the same mesh-free method that is used in this paper [21-23]. Sladek et al. [24] used meshless local Petrov-Galerkin (MLPG) method for stress analysis in two-dimensional (2D), anisotropic and linear elastic/viscoelastic solids with continuously varying material properties. They adopted moving least squares (MLS) method for approximating the physical quantities in the local boundary integral equations (LBIEs). Also several analyses have been carried out about free vibration of continuously graded fiber-reinforced cylindrical shells or panels based on the three-dimensional theory of elasticity, using differential quadrature method [25-27]. Chen et al. [28] studied free vibration of simply supported, fluid-filled orthotropic functionally graded cylindrical shells based on the three-dimensional fundamental equations of anisotropic elasticity.

In the present work a different Mesh-Free method was used for free vibration analysis of orthotropic FGM cylinders. The cylinders are assumed to be a mixture of two isotropic materials as fiber and matrix. The volume fraction of the fiber is changed in the radial direction. Then mechanical properties of these cylinders are changed in the radial direction. In this simulation, an axisymmetric model is applied and MLS shape functions are used for approximation of displacement field in the weak form of equilibrium equation, like as Element-Free Galerkin (EFG) but the transformation method was used for the imposition of essential boundary conditions. In the transformation method, after correction of mesh-free shape functions, essential boundary conditions are imposed as in the FEM. In this method, number of degrees of freedom does not increase unlike EFG.Effects of volume fraction exponent, geometrical parameters, and boundary conditions on natural frequencies in orthotropic FGM cylinders are investigated by the proposed model.

2 GOVERNING EQUATIONS

The weak form of equation of motion in the absence of external forces is expressed by the following relation [23]:

$$\int \sigma.\delta(\varepsilon)dv = -\int \rho(r)\ddot{u}.\delta u dv \tag{1}$$

In the above relation, σ, ε, u and $\ddot{u}$ are stress, strain, displacement and acceleration vectors respectively. For axisymmetric problems stress and strain vectors are as follows:

$$\sigma = \left[\sigma_r, \sigma_\theta, \sigma_z, \sigma_{rz}\right]^T \quad , \quad \varepsilon = \left[\varepsilon_r, \varepsilon_\theta, \varepsilon_z, \varepsilon_{rz}\right]^T \tag{2}$$

Stress vector is expressed in terms of strain vector by means of Hook's law:

$$\sigma = D\varepsilon \tag{3}$$

Matrix D is defined for an orthotropic cylinder as follows [23]:

$$\mathrm{D} = \begin{bmatrix} c_{11} & c_{12} & c_{13} & 0 \\ c_{12} & c_{22} & c_{23} & 0 \\ c_{13} & c_{23} & c_{33} & 0 \\ 0 & 0 & 0 & c_{55} \end{bmatrix} \tag{4}$$

where,

$$\begin{aligned} &c_{11} = \frac{1-\nu_{23}\,\nu_{32}}{E_2\,E_3\,\Delta} \quad , \quad c_{22} = \frac{1-\nu_{31}\,\nu_{13}}{E_1\,E_3\,\Delta} \quad , \quad c_{33} = \frac{1-\nu_{21}\,\nu_{12}}{E_1\,E_2\,\Delta} \quad , \; c_{55} = G_{12} \\ &c_{12} = \frac{\nu_{21}+\nu_{31}\,\nu_{23}}{E_2\,E_3\,\Delta} \quad , \quad c_{23} = \frac{\nu_{32}+\nu_{12}\,\nu_{31}}{E_1\,E_3\,\Delta} \quad , \quad c_{13} = \frac{\nu_{31}+\nu_{21}\,\nu_{32}}{E_2\,E_3\,\Delta} \\ &\Delta = \frac{1-\nu_{32}\nu_{23}-\nu_{21}\nu_{12}-\nu_{13}\nu_{31}-2\,\nu_{32}\nu_{21}\nu_{13}}{E_1E_2E_3} \end{aligned} \tag{5}$$

3 MESH-FREE NUMERICAL ANALYSIS

In these analyses moving least square shape functions introduced by Lancaster and Salkauskas [29] is used for approximation of displacement vector in the weak form of motion equation. Displacement vector u can be approximated by MLS shape functions as follows [23]:

$$u = \left[u_r, u_z\right]^T = \Phi\hat{u} \tag{6}$$

where $\hat{u}$ and Φ are virtual nodal values vector and shape functions matrix respectively.

$$\hat{\mathrm{u}} = \left[(\hat{u}_r)_1, (\hat{u}_z)_1, \ldots\ldots\ldots(\hat{u}_r)_N, (\hat{u}_z)_N\right]^T \tag{7}$$

and

$$\Phi = \begin{bmatrix} \Phi_1 & 0 & \Phi_2 & 0 & . & . & . & . & \Phi_N & 0 \\ 0 & \Phi_1 & 0 & \Phi_2 & . & . & . & . & 0 & \Phi_N \end{bmatrix} \tag{8}$$

N is total number of nodes and Φ_i is MLS shape function of node located at $\mathrm{X}(r,z) = \mathrm{X_i}$ and defined as follows [21]:

$$\Phi_i(\mathrm{X}) = \underbrace{\mathrm{P^T(X)}\left[\mathrm{H(X)}\right]^{-1} w(\mathrm{X}-\mathrm{X}_i)\mathrm{P}(\mathrm{X}_i)}_{(1\times1)} \tag{9}$$

In the above equation, w is cubic Spline weight function, P is base vector and H is moment matrix and are defined as follows:

$$\mathrm{P(X)} = [1, r, z]^T \tag{10}$$

$$\mathrm{H}(X)=\left[\sum_{i=1}^{n} w(X-X_i)P(X_i)P^T(X_i)\right] \tag{11}$$

By using Eq.(6) for approximation of displacement vector, strain vector can be expressed in terms of virtual nodal values:

$$\varepsilon = B\hat{u} \tag{12}$$

where matrix B is defined as follows [23]:

$$\mathrm{B}=\begin{bmatrix} \frac{\partial\Phi_1}{\partial r} & 0 & \frac{\partial\Phi_2}{\partial r} & 0 & \ldots & \frac{\partial\Phi_N}{\partial r} & 0 \\ \frac{\Phi_1}{r} & 0 & \frac{\Phi_2}{r} & 0 & \ldots & \frac{\Phi_N}{r} & 0 \\ 0 & \frac{\partial\Phi_1}{\partial z} & 0 & \frac{\partial\Phi_2}{\partial z} & \ldots & 0 & \frac{\partial\Phi_N}{\partial z} \\ \frac{\partial\Phi_1}{\partial z} & \frac{\partial\Phi_1}{\partial r} & \frac{\partial\Phi_2}{\partial z} & \frac{\partial\Phi_2}{\partial r} & \ldots & \frac{\partial\Phi_N}{\partial z} & \frac{\partial\Phi_N}{\partial r} \end{bmatrix} \tag{13}$$

Substitution of Eqs.(3), (6) and (12) in Eq. (1) leads to:

$$M\ddot{\hat{u}} + K\hat{u} = 0 \tag{14}$$

where

$$\mathrm{M}=\int \rho\Phi^T\Phi dv \qquad \mathrm{k}=\int \mathrm{B}^T\mathrm{D}\mathrm{B}dv \tag{15}$$

For numerical integration, problem domain is discretized to a set of background cells with gauss points inside each cell. Then global stiffness matrix **k** is obtained numerically by sweeping all gauss points.

Imposition of essential boundary conditions in the system of Eq.(14) is not possible. Because MLS shape functions don't satisfy the Kronecker delta property. In this work transformation method is used for imposition of essential boundary conditions. For this purpose transformation matrix is formed by establishing relation between nodal displacement vector U and virtual displacement vector $\hat{u}$.

$$U = T\hat{u} \tag{16}$$

T is the transformation matrix and is defined [23]:

$$\mathrm{T}=\begin{bmatrix} \Phi_1(x_1) & 0 & \Phi_2(x_1) & 0 & \ldots & \Phi_N(x_1) & 0 \\ 0 & \Phi_1(x_1) & 0 & \Phi_2(x_1) & \ldots & 0 & \Phi_N(x_1) \\ \vdots & \vdots & \vdots & \vdots & \ldots & \vdots & \vdots \\ \Phi_1(x_N) & 0 & \Phi_2(x_N) & 0 & \ldots & \Phi_N(x_N) & 0 \\ 0 & \Phi_1(x_N) & 0 & \Phi_2(x_N) & \ldots & 0 & \Phi_N(x_N) \end{bmatrix} \tag{17}$$

By using Eq. (16) system of linear Eq. (14) can be rearranged to:

$$\hat{M}\ddot{U} + \hat{K}U = 0 \tag{18}$$

where

$$\hat{M} = T^{-T} M T^{-1}, \hat{K} = T^{-T}.K.T^{-1} \tag{19}$$

Now the essential B. Cs. can be enforced to the modified equations system (18) easily like the finite element method. Solving this eigenvalue problem, natural frequencies and mode shapes of the cylinder are determined.

4 MATERIAL PROPERTIES IN ORTHOTROPIC FGM CYLINDERS

Consider an orthotropic cylinder with inner radius r_i, outer radius r_o, and length L. This cylinder is assumed a mixture of fiber that is embedded in matrix. With changing fiber density in the radial direction, the cylinder will be orthotropic and FGM. The effective mechanical properties of the orthotropic cylinders are obtained based on a micromechanical model as follows [30-31]:

$$E_{11} = V_f E_{11}^f + V_m E_{11}^m \tag{20}$$

$$\frac{1}{E_{ii}} = \frac{V_f}{E_{ii}^f} + \frac{V_m}{E_{ii}^m} - V_f V_m \frac{\upsilon_f^2 E_{ii}^m / E_{ii}^f + \upsilon_m^2 E_{ii}^f / E_{ii}^m - 2\upsilon^f \upsilon^m}{V_f E_{ii}^f + V_m E_{ii}^m} \quad (i = 2,3) \tag{21}$$

$$\frac{1}{G_{ij}} = \frac{V_f}{G_{ij}^f} + \frac{V_m}{G_{ij}^m} \quad (ij = 12,13 \text{ and } 23) \tag{22}$$

$$\upsilon_{ij} = V_f \upsilon^f + V_m \upsilon^m \quad (ij = 12,13 \text{ and } 23) \tag{23}$$

$$\rho = V_f \rho^f + V_m \rho^m \tag{24}$$

where E_{ii}^f, G_{ij}^f, υ^f and ρ^f are elasticity modulus, shear modulus, Poisson's ratio and density, of the fiber, and E_{ii}^m, G_{ij}^m, υ^m and ρ^m are corresponding properties for the matrix constituent. V_f and V_m are the fiber and matrix volume fractions. The profile of the variation of the fiber volume fraction has important effects on the cylinder behavior. Several models have been proposed for the variation of material properties. In this paper, to show the flexibility of the proposed Mesh-Free model, two profiles for the variation of volume fraction of fiber are considered.

4.1 Simple power model

In this model, variation of volume fraction of fiber, V_f, along the cylinder radius is presented by a simple power function as follows [8]:

$$V = V_{fi} \left(\frac{r}{r_i} \right)^n, \quad n = ln\left(\frac{V_{fo}}{V_{fi}} \right) / ln\left(\frac{r_o}{r_i} \right) \tag{25}$$

where V_{fi} and V_{fo} are the volume fraction of the fiber on the inner and outer surfaces, respectively.

4.2 Volume fraction model

In this model, volume fraction of fiber, V_f, vary along the radial direction as follows [8]:

$$V_f = V_{fi} + \left(V_{fo} - V_{fi} \right) \left(\frac{r^n - r_i^n}{r_o^n - r_i^n} \right) \tag{26}$$

where n is a real number except zero. Fig.1 shows variation of volume fraction of the fiber along the radius according to volume fraction model for various values of n.

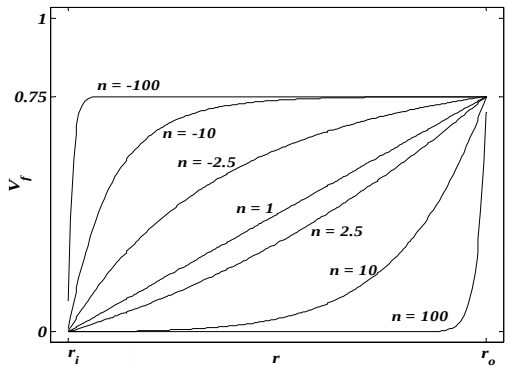

Fig. 1
Variation of volume fraction of the fiber from zero to 0.75 along the radius according to volume fraction model.

5 RESULTS AND DISCUSSIONS

In this work for all finite element (FE) simulations, rectangular four-node axisymmetric elements are used. Grid arrangements in FE simulations are similar to those of Mesh-Free simulations. So, the number of elements in FE simulations is equal to the number of integral cells in similar Mesh-Free simulations. To compare the results of Mesh-Free analyses and FE analyses, the same grid arrangements were used in these two types of analyses. For this reason, regular grid arrangements were used in all simulations although irregular grid arrangements can be used for Mesh-Free simulations easily. Fig.2 shows Schematic sketch of the Clamped-Clamped axisymmetric cylinder with background cells, gauss points and nodes arrangements.

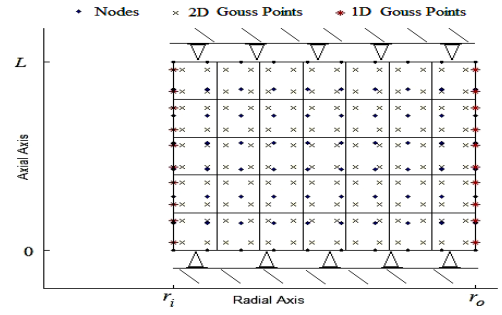

Fig. 2
Schematic sketch of the Clamped-Clamped axisymmetric cylinder.

For validation of the proposed model, a homogeneous solid cylinder with $L/r_o = 4$ and $\upsilon = 0.3$ is considered. The two ends of the cylinder are assumed to be free. Table 1. shows the first five frequency parameters obtained from the proposed Mesh-Free method and FEM for three different grid arrangements and compared with results of references [9], [13] and [11,12]. In Table 1, the frequency parameters are defined by [13]:

$$\Omega = \omega r_o \sqrt{\rho / G} \tag{27}$$

In this definition, ω, ρ, and G are natural frequency, density, and shear modulus, respectively. It is obvious from Table1. that results from both Mesh-Free method and FEM have very good accuracy. In addition, the proposed model is a little more accurate than the FEM, especially for higher frequencies.

Table 1
First five frequency parameters for a isotropic free–free solid cylinder, ($L / r_0 = 4$)

Grid Arrangement	solutions	Ω_1	Ω_2	Ω_3	Ω_4	Ω_5
5*15	Mesh-Free	1.24700664	2.92043586	3.02841227	3.82432182	4.18564068
	FEM	1.24937244	2.89736006	2.99489762	3.84032298	4.19555697
10*30	Mesh-Free	1.24699705	2.92029741	3.02823280	3.82398949	4.18480418
	FEM	1.24758825	2.91703138	3.01924495	3.82910988	4.19017043
20*60	Mesh-Free	1.24699467	2.92028254	3.02820750	3.82394895	4.18471717
	FEM	1.24714245	2.91959585	3.02595877	3.82529721	4.18620930
References	[13]	1.24699388	2.92027959	3.02820195	3.82393930	4.18469813
	[11,12]	1.24699388	2.92018985	3.02820178	3.82393928	4.18469780
	[9]	1.24699	2.92028	3.02820	3.82394	4.18470

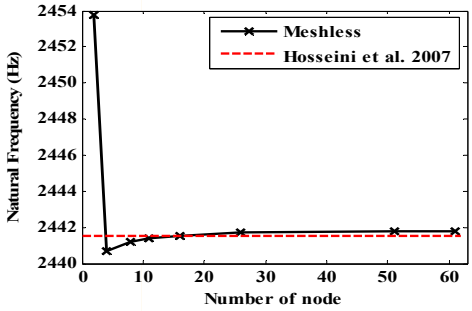

Fig. 3
Convergence of first natural frequency of the FGM cylinder in plane strain state for different number of node arrangement.

At second step of validation, an FGM cylinder in plane strain state is considered like as Hosseini et.al [16] and the convergence rate of the proposed model is examined. Fig.3 shows a comparison between numerical results of proposed method with different number of node arrangements and results that reported by Hosseini et.al [16]. This figure shows a good convergence rate for the proposed Mesh-Free method. After the validation of the proposed model, various models of orthotropic FGM cylinders are analyzed. In these cylinders silicon carbide (SiC) is considered as the fiber and stainless steel (SUS304) is considered as the matrix. Mechanical properties of these materials are summarized in Table 2. Parameter frequency of these analyses is defined by:

$$\Omega = \omega r_o \sqrt{\rho_m / G_m} \tag{28}$$

In this definition, ρ_m and G_m are density and shear modulus of matrix (SUS304), respectively. In the first model of analysis, volume fraction of the fiber increases along the radius according to volume fraction model from zero to 75%, also end conditions of FGM cylinders are assumed to be clamped–free. This analysis is done for isotropic cylinders (pure SiC and SUS304), continuous orthotropic cylinder with 75% fiber and 25% matrix and orthotropic FGM cylinders that volume fraction of the fiber is changed from zero in the inner radius to 75% in outer according to volume fraction model. Results obtained from this analysis are summarized in Table 3.

In this table, the effect of volume fraction exponent (n) on natural frequencies is investigated. Table 3 reveals that the more n have the lower natural frequencies, because increasing n leads to decrease the fiber volume fraction (see Fig.1). So, natural frequency can be controlled by the choice of proper volume fraction exponent (n). Natural frequencies of the orthotropic FGM and orthotropic homogeneous cylinders lie between the natural frequencies of the similar isotropic SiC cylinder and those of the similar isotropic stainless steel cylinder, as expected.

Table 2
Mechanical properties of silicon carbide (SiC) and stainless steel (SUS304) [8]

Material	Properties		
	E(GPa)	V	ρ (kg/m^3)
Silicon carbide (SiC)	427	0.17	3210
Stainless steel (SUS304)	207.78	0.3177	8166

Table 3
First five frequency parameters for free–clamped orthotropic FGM cylinder with variation of volume fraction of the fiber from zero to 75% along the radius according to volume fraction model ($r_o / r_i = 2$, $L / r_o = 3$)

	solutions	SiC	SUS (25%)/ SiC (75%)	*n = -10*	*n = -2.5*	*n = 1*	*n = 2.5*	*n = 10*	SUS304
Ω_1	Mesh-Free	1.9482	1.5460	1.4670	1.3162	1.1814	1.1268	0.9757	0.8576
	FEM	1.9482	1.5460	1.4675	1.3163	1.1813	1.1266	0.9753	0.8575
Ω_2	Mesh-Free	4.9842	3.8112	3.5300	3.0837	2.7439	2.6180	2.3086	2.1216
	FEM	4.9833	3.8105	3.5318	3.0833	2.7431	2.6171	2.3075	2.1214
Ω_3	Mesh-Free	5.0281	3.8613	3.5577	3.1488	2.8306	2.7117	2.4150	2.2209
	FEM	5.0246	3.8586	3.5576	3.1475	2.8289	2.7098	2.4126	2.2191
Ω_4	Mesh-Free	5.5486	4.2781	3.9289	3.4543	3.1031	2.9756	2.6711	2.4890
	FEM	5.5460	4.2761	3.9304	3.4537	3.1020	2.9743	2.6693	2.4880
Ω_5	Mesh-Free	6.0932	4.8470	4.6054	4.1125	3.6888	3.5282	3.1225	2.8166
	FEM	6.0937	4.8475	4.6083	4.1142	3.6896	3.5286	3.1216	2.8164

The second model is a cylinder similar to the first model, except that the volume fraction of the fiber decreases along the radius from 75% to zero. Results obtained from this analysis are summarized in Table 4.

In this table, the effect of volume fraction exponent (n) on natural frequencies is investigated too. Table 4. reveals that the more n have the higher natural frequencies, because increasing of n increases SiC volume fraction. Also, natural frequencies of the orthotropic FGM and only orthotropic cylinder lie between the natural frequencies of the similar isotropic SiC cylinder and those of the similar isotropic stainless steel cylinder too. It is obvious from Tables 3. and 4 that the natural frequencies of the orthotropic FGM cylinders are close to those of an isotropic cylinder with dominant component material.

The third model is a cylinder similar to the first model, except that this cylinder is longer than the first model, so that $L/r_o = 6$. Results obtained from this analysis are summarized in Table 5., Fig. 4 shows first frequency parameters for continuous orthotropic cylinder with 75% fiber and also for orthotropic FGM cylinders that volume fraction of the fiber is changed from zero in the inner radius to 75% in outer according to Eq. (26) with different values of the exponents, $n = -10, 1, 10$, versus different values of the ratios of length to outer radius, L / r_o. In the mentioned cylinders the ratios of radii is equal to, $r_o / r_i = 2$. In Fig. 4 and by comparing Tables 3. and 5 reveals that increasing of the cylinder length decreases natural frequencies of the orthotropic FGM cylinder because the stiffness of system is reduced, as homogeneous cylinders. This trend is observed for the isotropic cylinders too.

Table 4
First five frequency parameters for free–clamped orthotropic FGM cylinder with variation of volume fraction of the fiber from 75% to zero along the radius according to volume fraction ($r_o / r_i = 2$, $L / r_o = 3$)

	solutions	SUS304	*n = -10*	*n = -2.5*	*n = 1*	*n = 2.5*	*n = 10*	SUS (25%)/ SiC (75%)	SiC
Ω_1	Mesh-Free	0.8576	0.9023	1.0015	1.1133	1.1669	1.3508	1.5460	1.9482
	FEM	0.8575	0.9018	1.0013	1.1133	1.1670	1.3513	1.5460	1.9482
Ω_2	Mesh-Free	2.1216	2.2725	2.5255	2.7943	2.9225	3.3613	3.8112	4.9842
	FEM	2.1214	2.2703	2.5245	2.7936	2.9219	3.3614	3.8105	4.9833
Ω_3	Mesh-Free	2.2209	2.3853	2.6527	2.9284	3.0570	3.4762	3.8613	5.0281
	FEM	2.2191	2.3809	2.6501	2.9265	3.0552	3.4753	3.8586	5.0246
Ω_4	Mesh-Free	2.4890	2.6766	2.9612	3.2541	3.3913	3.8431	4.2781	5.5486
	FEM	2.4880	2.6727	2.9590	3.2523	3.3897	3.8424	4.2761	5.5460
Ω_5	Mesh-Free	2.8166	2.9644	3.2226	3.5195	3.6668	4.2000	4.8470	6.0932
	FEM	2.8164	2.9625	3.2222	3.5200	3.6676	4.2028	4.8475	6.0937

Table 5
First five frequency parameters for free–clamped orthotropic FGM cylinder with variation of volume fraction of the fiber from zero to 75% along the radius according to volume fraction model ($r_o / r_i = 2$, $L / r_o = 6$)

	solutions	SiC	SUS (25%)/ SiC (75%)	*n = -10*	*n = -2.5*	*n = 1*	*n = 2.5*	*n = 10*	SUS304
Ω_1	Mesh-Free	0.9734	0.7724	0.7335	0.6590	0.5918	0.5645	0.4882	0.4277
	FEM	0.9734	0.7724	0.7338	0.6590	0.5917	0.5644	0.4879	0.4276
Ω_2	Mesh-Free	2.9019	2.2952	2.1708	1.9378	1.7326	1.6504	1.4262	1.2564
	FEM	2.9028	2.2958	2.1723	1.9385	1.7329	1.6506	1.4259	1.2566
Ω_3	Mesh-Free	4.6011	3.5541	3.2823	2.8635	2.5379	2.4156	2.1079	1.9118
	FEM	4.6021	3.5541	3.2835	2.8627	2.5367	2.4144	2.1068	1.9119
Ω_4	Mesh-Free	4.9859	3.8160	3.5403	3.1171	2.7804	2.6548	2.3475	2.1660
	FEM	4.9771	3.8098	3.5380	3.1149	2.7780	2.6524	2.3450	2.1642
Ω_5	Mesh-Free	5.1258	3.9325	3.6144	3.1757	2.8480	2.7265	2.4249	2.2333
	FEM	5.1177	3.9262	3.6106	3.1703	2.8429	2.7215	2.4197	2.2283

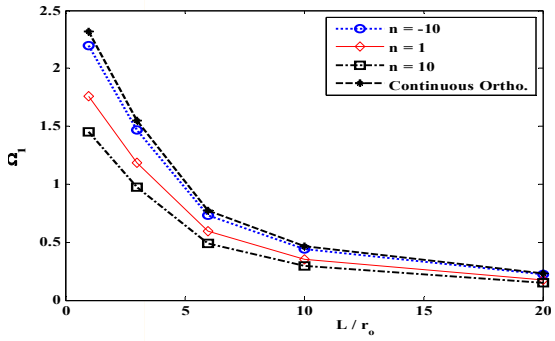

Fig. 4
First frequency parameters versus different values of L/r_0 for free–clamped continuous and FGM orthotropic cylinders with $r_0/r_i = 2$.

The fourth model is a cylinder similar to that of the first model, except that this one is thinner with, $r_o/r_i = 1.5$. Results obtained from free vibration analysis of this cylinder are shown in Table 6., Fig. 5 shows first frequency parameters for continuous orthotropic cylinder with 75% fiber and also for orthotropic FGM cylinders that volume fraction of the fiber is changed from zero to 75% in along the radial direction according to Eq. (26) with different values of the exponents, $n = -10, 1, 10$, versus different values of the ratios of radii, r_o/r_i, for the ratios of length to outer radius of, $L/r_o = 3$.

Table 6
First five frequency parameters for free–clamped orthotropic FGM cylinder with variation of volume fraction of the fiber from zero to 75% along the radius according to volume fraction model ($r_o / r_i = 1.5$, $L / r_o = 3$)

	solutions	SiC	SUS (25%)/ SiC (75%)	*n = -10*	*n = -2.5*	*n = 1*	*n = 2.5*	*n = 10*	SUS304
Ω_1	Mesh-Free	1.9462	1.5438	1.3810	1.2451	1.1650	1.1321	1.0102	0.8544
	FEM	1.9462	1.5438	1.3813	1.2452	1.1649	1.1320	1.0099	0.8543
Ω_2	Mesh-Free	4.4596	3.4036	2.9740	2.6567	2.4831	2.4145	2.1763	1.9207
	FEM	4.4588	3.4030	2.9746	2.6566	2.4827	2.4140	2.1755	1.9205
Ω_3	Mesh-Free	4.5147	3.4594	3.0081	2.6983	2.5300	2.4637	2.2334	1.9851
	FEM	4.5119	3.4572	3.0069	2.6966	2.5283	2.4619	2.2314	1.9835
Ω_4	Mesh-Free	4.8493	3.7290	3.2232	2.8885	2.7100	2.6404	2.4032	2.1578
	FEM	4.8460	3.7267	3.2227	2.8874	2.7087	2.6390	2.4016	2.1568
Ω_5	Mesh-Free	5.7351	4.4330	3.8244	3.4220	3.2060	3.1214	2.8318	2.5069
	FEM	5.7359	4.4338	3.8270	3.4233	3.2067	3.1220	2.8316	2.5070

In Fig. 5 and by comparing Tables 3 and 6 reveals that in the negative values of the volume fraction exponents, increasing of the thickness of orthotropic FGM cylinders decreases the first frequencies parameters, while in the positive values is inversely. It also reveals that second and more frequencies parameters increase by increasing the wall thickness of orthotropic FGM cylinder.

Finally, for investigation of boundary conditions effect on the natural frequencies, a different orthotropic FGM cylinder is considered. In this cylinder volume fraction of the fiber increases along the radius from 10% to 75% according to the simple power model Eq. (25).

Natural frequencies of this cylinder, are calculated by the proposed model under three different types of boundary conditions. Results obtained from these analyses are shown in Table 7. As seen in this table, for the clamped–clamped boundary condition, natural frequencies have the highest values in comparison with two other cases of boundary conditions. In addition, it is obvious from this table that the difference between three cases is reduced at higher frequencies.

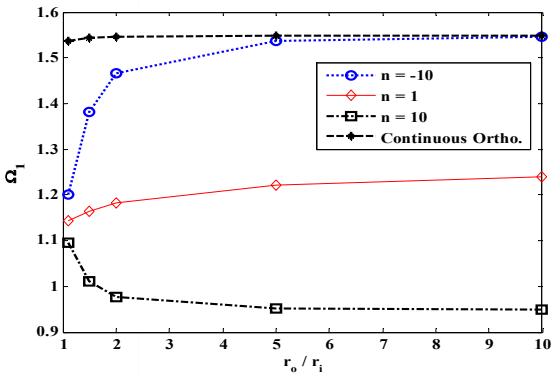

Fig. 5
First frequency parameters versus different values of r_0/r_i for free–clamped continuous and FGM orthotropic cylinders with $L/r_0 = 3$.

Table 7
First five frequency parameters for orthotropic FGM cylinder with variation of volume fraction of the fiber from 10% to 75% along the radius according to the simple power model for different boundary conditions ($r_o / r_i = 2$, $L / r_o = 3$)

boundary condition	solutions	Ω_1	Ω_2	Ω_3	Ω_4	Ω_5
Clamped–Clamped	Mesh-Free	2.2892	2.8962	3.2312	3.6562	4.5679
	FEM	2.2889	2.8954	3.2301	3.6577	4.5770
Clamped-Free	Mesh-Free	1.1617	2.7187	2.8001	3.0801	3.6529
	FEM	1.1615	2.7178	2.7981	3.0787	3.6532
Free-Free	Mesh-Free	2.1531	2.7548	2.8044	2.9878	3.0959
	FEM	2.1530	2.7540	2.8022	2.9843	3.0950

6 CONCLUSIONS

In this study, the free vibrations of orthotropic FGM cylinders is analyzed with a Mesh-Free and finite element method. The cylinders are assumed to be combination of two isotropic materials. The volume fraction of the fiber is changed in the radial direction. In this simulation, an axisymmetric model is used. Proposed Mesh-Free method is based on MLS shape functions and the weak form equation of motion. Essential boundary conditions are imposed by transfer function method. In this study, effect of geometric dimensions, type of boundary condition and volume fraction exponent on natural frequencies were investigated and following results were obtained.

- Both Mesh-Free and the finite element method have good accuracy in solving this problem.
- Mesh-Free method in comparison with FEM has more accuracy in solving this problem, especially for higher frequencies.
- In orthotropic FGM cylinders, frequency values are close to the frequencies of isotropic cylinder made of dominant material.

- Increasing of the cylinder thickness of orthotropic FGM cylinders has different effects on first frequency parameter, but lead to increasing on the values of second or more frequency parameter.
- Type of boundary conditions has considerable effect on the frequency values.
- Natural frequency of orthotropic FGM cylinders can be controlled by the choice of proper volume fraction exponent, *n*.

REFERENCES

[1] Koizumi M., 1993, The concept of FGM, *Ceramic Transactions Functionally Graded Materials* **34**:3-10.

[2] Kashtalyan M., 2004, Three-dimensional elasticity solution for bending of functionally graded rectangular plates, *European Journal of Mechanics A–Solid* **23**:853-864.

[3] Loy C.T., Lam K.Y., Reddy J.N., 1999, Vibration of functionally graded cylindrical shells, *International Journal of Mechanical Sciences* **41**:309-324.

[4] Pradhan S.C., Loy C.T., Reddy J.N., 2000, Vibration characteristics of functionally graded cylindrical shells under various boundary conditions, *Applied Acoustics* **61**:111-129.

[5] Kadoli R., Ganesan K., 2006, Buckling and free vibration analysis of functionally graded cylindrical shells subjected to a temperature-speciefied boundary condition, *Journal of Sound and Vibrations* **289**:450-480.

[6] Haddadpour H., Mahmoudkhani S., Navazi H.M., 2007, Free vibration analysis of functionally graded cylindrical shells including thermal effects, *Thin-walled structures* **45**:591-599.

[7] Ansari R., Darvizeh M., 2008, Prediction of dynamic behavior of FGM shells under arbitrary boundary conditions, *Composite Structures* **85**:284-292.

[8] Mollarazi H.R., Foroutan M., Moradi-Dastjerdi R., 2011, Analysis of free vibration of functionally graded material (FGM) cylinders by a meshless method, *Journal of Composite Materials* **46**:507-515.

[9] Leissa A.W., So J., 1995, Accurate vibration frequencies of circular cylinders from three dimensional analysis, *Journal of the Acoustical Society of America* **98**:2136-2141.

[10] Leissa A.W., So J., 1995, Comparisons of vibration frequencies for rods and beams from 1D and 3D analysis, *Journal of the Acoustical Society of America* **98**:2122-2135.

[11] Hutchinson J.R., 1996, Accurate vibration frequencies of circular cylinders from three-dimensional analysis, *Journal of the Acoustical Society of America* **98**:2136-2141.

[12] Hutchinson J.R., 1995, Accurate vibration frequencies of circular cylinders from three-dimensional analysis, *Journal of the Acoustical Society of America* **100**:1894-1895.

[13] Zhou D., Cheung Y.K., Lo S.H., Au F.T.K., 2003, 3D vibration analysis of solid and hollow circular cylinders via Chebyshev–Ritz method, *Computer Methods in Applied Mechanics and Engineering* **192**:1575-1589.

[14] Han X., Liu G.R., Xi Z.C., Lam K.Y., 2001, Transient waves in a functionally graded cylinder, *International Journal of Solids and Structures* **38**:3021-3037.

[15] Shakeri M., Akhlaghi M., Hoseini S.M., 2006, Vibration and radial wave propagation velocity in functionally graded thick hollow cylinder, *Composite Structures* **76**:174-181.

[16] Hosseini S.M., Akhlaghi M., Shakeri M., 2007, Dynamic response and radial wave propagation velocity in thick hollow cylinder made of functionally graded materials, *International Journal for Computer-Aided Engineering and Software* **24**:288-303.

[17] Asgari M., Akhlaghi M., Hosseini S.M., 2009, Dynamic analysis of two-dimensional functionally graded thick hollow cylinder with finite length under impact loading, *Acta Mechanica* **208**:163-180.

[18] Hosseini S.M., Abolbashari M.H., 2010, General analytical solution for elastic radial wave propagation and dynamic analysis of functionally graded thick hollow cylinders subjected to impact loading, *Acta Mechanica* **212**:1-19.

[19] Shahabian F., Hosseini S.M., 2010, Stochastic dynamic analysis of a functionally graded thick hollow cylinder with uncertain material properties subjected to shock loading, *Material & Design* **31**:894-901.

[20] Zhang G.M., Batra R.C., 2007, Wave propagation in functionally graded materials by modified smoothed particle hydrodynamics (MSPH) method, *Journal of Computational Physics* **222**:374-390.

[21] Foroutan M., Moradi-Dastjerdi R., 2011, Dynamic analysis of functionally graded material cylinders under an impact load by a mesh-free method, *Acta Mechanica* **219**:281-290.

[22] Foroutan M., Moradi-Dastjerdi R., Sotoodeh-Bahreini R., 2012, Static analysis of FGM cylinders by a mesh-free method, *Steel and Composite Structures* **12**:1-11.

[23] Moradi-Dastjerdi R., Foroutan M., Pourasghar A., 2013, Dynamic analysis of functionally graded nanocomposite cylinders reinforced by carbon nanotube by a mesh-free method, *Material & Design* **44**:256-266.

[24] Sladek J., Sladek V., Zhang Ch., 2005, Stress analysis in anisotropic functionally graded materials by the MLPG method, *Engineering Analysis with Boundary Elements* **29**:597-609.

[25] Yas M.H., Garmsiri K., 2010, Three-dimensional free vibration analysis of cylindrical shells with continuous grading reinforcement, *Steel and Composite Structures* **10**:349-360.

[26] Sobhani Aragh B., Yas M.H., 2010, Static and free vibration analyses of continuously graded fiber-reinforced cylindrical shells using generalized power-law distribution, *Acta Mechanica* **215**:155-173.

[27] Sobhani Aragh B., Yas M.H., 2010, Three-dimensional free vibration of functionally graded fiber orientation and volume fraction cylindrical panels, *Material & Design* **31**:4543-4552.
[28] Chen W.Q., Bian Z.G., Ding H.J., 2004, Three-dimensional vibration analysis of fluid-filled orthotropic FGM cylindrical shells, *International Journal of Mechanical Sciences* **46**:159-171.
[29] Lancaster P., Salkauskas K., 1981, Surface generated by moving least squares methods, *Mathematics of Computation* **37**:141-158.
[30] Shen H.S., 2009, A comparison of buckling and post buckling behavior of FGM plates with piezoelectric fiber reinforced composite actuators, *Composite Structures* **91**:375-384.
[31] Vasiliev V.V., Morozov E.V., 2001, *Mechanics and Analysis of Composite Materials*, Elsevier Science Ltd, First Edition.